DETECTION OF NITROGEN DEFICIENCY IN POTATOES USING SMALL UNMANNED AIRCRAFT SYSTEMS

E.R. Hunt Jr.

Hydrology and Remote Sensing Laboratory
USDA-ARS
Beltsville, Maryland

D.A. Horneck and P.B. Hamm

Hermiston Agricultural Research and Extension Center
Oregon State University
Hermiston, Oregon

D.J. Gadler, A.E. Bruce, R.W. Turner, and C.B. Spinelli

Engineering, Operations and Technology
Boeing Research and Technology
Kent, Washington

J.J. Brungardt

Paradigm ISR
Bend, Oregon

ABSTRACT

Small Unmanned Aircraft Systems (sUAS) are recognized as potentially important remote-sensing platforms for precision agriculture. A nitrogen rate experiment was established in 2013 with 'Ranger Russet' potatoes by applying four rates of nitrogen fertilizer (112, 224, 337, and 449 kg N/ha) in a randomized block design with 3 replicates. A Tetracam Hawkeye sUAS and Agricultural Digital Camera Lite sensor were used to collect imagery with near-infrared (NIR), red and green bands with pixel sizes from 1 to 4 cm. Colored tarps were set out for each flight for an empirical calibration of digital numbers to spectral reflectances; however, the camera footprint was too small to have the tarps in each image. Two spectral indices were calculated from the color-infrared imagery, the normalized difference vegetation index (NDVI) and the green normalized difference vegetation index (GNDVI). NDVI and GNDVI from the tarp digital numbers were correlated to NDVI and GNDVI calculated from tarp spectral reflectances. The slopes and intercepts of the calibration equations varied

with the exposure time, which was set by the sensor. For images without the tarps, the exposure time was used to determine which calibration equation was used. Variation of NDVI and GNDVI over the growing season followed changes of leaf area index or plant cover. Comparison of GNDVI with NDVI was expected to enhance sensitivity to differences of leaf chlorophyll content; but only plots with the low N treatment were detectable. The value of sUAS for precision agriculture is information and its relevance to management. A first law of precision agriculture is proposed, "it's the sensor, not the platform."

Keywords: Remote sensing, unmanned aerial vehicles, *Solanum tuberosum* L., leaf area index, leaf chlorophyll content, sensor calibration

INTRODUCTION

Remote sensing is generally considered an important geospatial technology for precision agriculture; however satellite images were frequently not useful because of large pixel sizes, infrequent revisit times, long waits between acquisition and delivery, and clouds. Small unmanned aircraft systems (sUAS) are seen as potential remote sensing platforms for precision agriculture, because low flight altitudes result in smaller pixel sizes (Herwitz et al., 2004; Hunt et al., 2005; Lelong et al., 2008; Zhang and Kovacs, 2012). In a report for the UAS trade group, the Association of Unmanned Vehicle Systems International (AUVSI), Jenkins and Vasigh (2013) conclude that the needs for agricultural remote sensing will lead to large increases in domestic UAS sales.

Many technologies for precision agriculture are deployed on ground-based vehicles, such as "on-the-go" nitrogen sensors (Shanahan et al., 2008). Aerial photography from manned aircraft is used to detect crop diseases (Johnson et al., 2003) and nitrogen deficiency (Blackmer et al., 1996; Scharf and Lory, 2002). So the question is not, are UAS useful for precision agriculture, but rather do UAS have better value compared to alternatives? Therefore, it was necessary to establish baselines of routine sUAS-image collection and analysis before comparisons were made with established technologies. We used these flights as an opportunity to conduct experiments for technology development and assessment, and not to establish better farming practices.

The main goal of precision farming is to reduce production costs while maintaining yields by applying fertilizer and pesticides when, where, and with the correct amounts that will provide the greatest benefit. Potatoes are a crop where both under- and over- fertilization of nitrogen cause problems with tuber yield and quality (Alva, 2004), so over-application of fertilizers as "insurance" is counterproductive. Furthermore, nutrients are stored underground in the developing tubers, so there may be few detectable changes aboveground that could be detected with remote sensing. Wu et al. (2006) found that nitrogen-deficiency in potatoes could be detected towards the end of the growing season with QuickBird imagery, but the cost of the imagery and interference by clouds limit the ability to make timely management decisions. Pixel sizes of Quickbird multispectral data are 2.44 m, so these pixels are still spectral mixtures of leaves,

soil and shadows. Our hypothesis is that sUAS imagery would help better manage potatoes because having fewer mixed pixel sizes would increase sensitivity to changes in growth and leaf chlorophyll contents (Hunt et al., in press). We tested this hypothesis by varying the amount of nitrogen to irrigated potatoes and compared growth and chlorophyll contents with imagery acquired with a small UAS.

METHODS

Experimental design and field measurements

The study was conducted at Oregon State University's Hermiston Agricultural Research and Extension Center (HAREC) in the Columbia River Basin. HAREC is located at 45.81944°N and 119.28333°W, at an elevation of 180 m. The average annual precipitation is 266 mm, with 51 mm during the growing season, so all crops rely on irrigation. July is the hottest month with average high and low temperatures of 32°C and 14°C, respectively. The soil type is a Hermiston Silt Loam (Coarse-silty, mixed, superactive, mesic Cumulic Haploxeroll).

A fertilization experiment with potatoes (*Solanum tuberosum* L. 'Ranger Russet') was established using a randomized block design with 4 rates of nitrogen fertilizer and 3 replications for a total of 12 plots (Fig. 1). Slow-release coated urea (ESN, Agrium Advanced Technologies, Loveland, CO) was applied on 25 April 2013. Each plot was 12 rows wide, with a row spacing of 87 cm. Based on the soil type, the potato variety, and the long growing season, the typical rate of N application at this location is 337 kg/ha (= 300 lbs/acre).

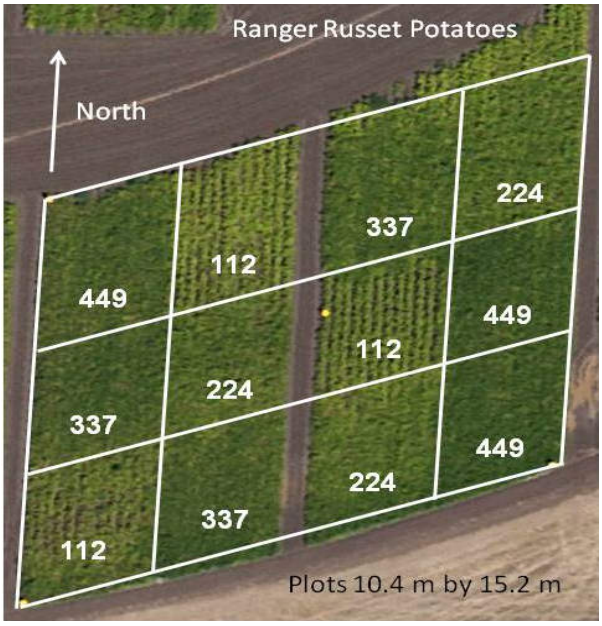

Fig. 1. Different rates of nitrogen fertilizer (kg/ha) were applied to irrigated potatoes ('Ranger Russet') at the Oregon State University's Hermiston Agricultural Research and Extension Center (HAREC). The image is a true-color aerial photograph acquired on 25 July 2013 (pixel size was about 8 cm).

Plant nitrogen status was determined using several methods. On 22 June and 5 August 2013, leaf chlorophyll concentrations were estimated using a Konica-Minolta SPAD-502 meter (Osaka, Japan). Furthermore, chlorophyll concentrations were measured for 1-cm leaf disks after extraction with dimethyl sulfoxide (Hunt and Daughtry, 2014). Petiole nitrate concentration was determined for 20 leaves (fourth leaf from top) on 1 June and the two dates above. LAI was measured using a Decagon Devices (Pullman, WA) AccuPAR model LP-80.

Image acquisition and analysis

A Tetracam, Inc. (Chatworth, CA) Hawkeye parafoil (Fig. 2) was selected for this study because its open design and large payload capacity allowed different sensors to be flown and tested. The sensor was a Tetracam Agricultural Digital Camera Lite (ADC-Lite) for acquiring color-infrared aerial photographs. The camera has a red-green-blue Bayer pattern filter, but without a hot mirror filter to block NIR from the CMOS detector. A yellow filter is added to remove blue light, so the blue channel records the NIR digital number (DN). We created our own color correction matrix for Tetracam's PixelWrench software based on soil color. The DN for the green and red channels included NIR, so the blue channel DN is used to subtract the NIR component from each band in PixelWrench. The focal length of the lens was 8.5 mm, exposure time was automatic, and the other camera settings were kept constant over the growing season. Images were saved in the 10-bit raw format and converted to TIFF images without gamma or white balance corrections.

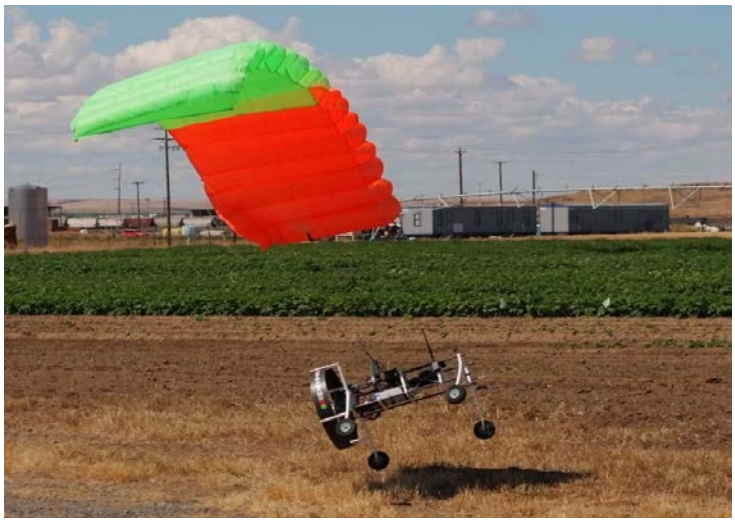

Fig. 2. A Tetracam small Unmanned Aircraft System (sUAS) is shown taking off with a Tetracam Agricultural Digital Camera Lite for acquisition of near-infrared (NIR), red, and green images.

The color-infrared photographs from the sUAS were not georegistered or stitched together. Instead, photographs were selected and examined individually

for coverage of the experimental plots. With the ExelisVIS (Boulder, Colorado) program, Environment for Visualizing Images (ENVI), each plot in one picture was outlined as a "Region of Interest", and mean digital numbers (DN) were determined. When a single plot was found on multiple images, DN from most nadir image were used.

We set out five tarps with different colors (Fig. 3) to calibrate DN using an empirical line with targets of known reflectance (Moran et al., 2003). Because of the low sUAS altitude above ground level during flight, almost all photos missed the tarps during a single flight. On several days, the sUAS missed the tarps completely. With rapid changes in the incident light level, tarp DN varied so calibration with an empirical line was not successful. We tried adjusting DN based on incident solar radiation measured every five minutes at the HAREC weather station (http://solardata.uoregon.edu/Hermiston.html), but the results were not good.

Fig. 3. Calibration tarps were set out for each flight. Tarps were 2.8 m by 2.8 m.

Another method for reducing the effects of varying light on DN is the calculation of normalized difference spectral indices (Lebourgeois et al., 2008). From the NIR, red and green bands (Fig. 4), two spectral indices were calculated:

$$NDVI = (NIR - Red)/(NIR + Red) \quad [1]$$

$$GNDVI = (NIR - Green)/(NIR + Green) \quad [2]$$

where: NDVI is the widely-used normalized difference vegetation index (Tucker, 1979); and GNDVI is the green normalized difference vegetation index (Gitelson et al., 1996). For images that included the tarps, DN-based NDVI and GNDVI were compared to reflectance-based NDVI and GNDVI (Hunt et al., 2005, 2010) to calculate calibration equations and determine how calibrations changed over the growing season.

Spectral indices have different sensitivities to chlorophyll and LAI (Daughtry et al., 2000). Because NIR reflectance is not affected by changes in chlorophyll content, and the red reflectance is only minimally affected (Fig. 4), NDVI is a better estimate of LAI (Daughtry et al., 2000). The green reflectance is strongly affected by differences in chlorophyll content (Fig. 4); GNDVI is hypothesized to have more sensitivity to chlorophyll content than to LAI (Daughtry et al., 2000). We tested the hypothesis that the differential sensitivities of an index to chlorophyll and LAI could be used as a measure of the nitrogen status. The

differential sensitivity would be expressed as differences in the slope of a regression line between two spectral indices.

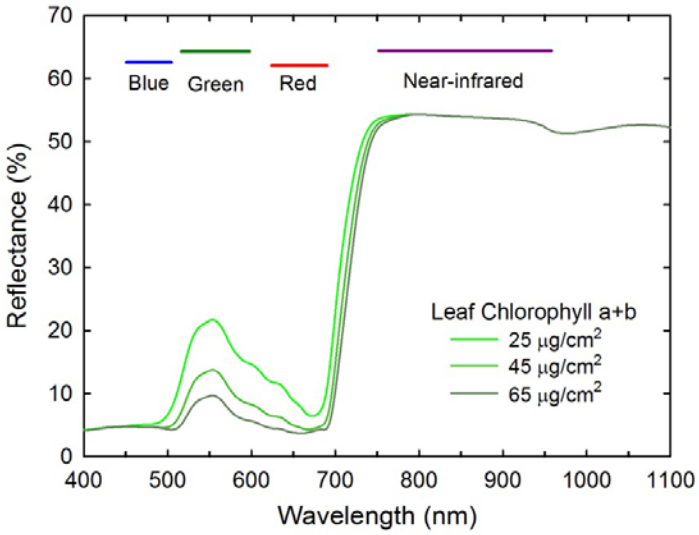

Fig. 4. Spectral reflectances of leaves were simulated with different chlorophyll contents using the PROSPECT leaf optics model (Feret et al., 2008). Along the top are the wavelength ranges of various multispectral bands.

Table 1. Treatment averages of leaf nitrogen and canopy measurements. Shaded cells indicate values that are significantly different from other N rates on that date.

Measurement	Applied nitrogen rate			
	112 kg/ha	224 kg/ha	337 kg/ha	449 kg/ha
Petiole NO_3 (%) 6/1	1.44	2.06	2.17	2.32
Petiole NO_3 (%) 6/22	0.54	1.21	1.40	1.57
Petiole NO_3 (%) 8/5	0.35	0.45	0.90	1.06
Chlorophyll (µg/cm^2) 6/22	20.9	25.8	23.1	28.8
Chlorophyll (µg/cm^2) 8/5	11.0	14.3	19.3	22.4
SPAD (value) 6/22	42.0	46.6	45.8	46.5
SPAD (value) 8/5	30.0	34.1	40.7	43.9
LAI (m^2/m^2) 6/22	2.0	3.0	3.3	3.4
LAI (m^2/m^2) 8/5	0.6	1.5	1.8	1.9

RESULTS AND DISCUSSION

At the beginning of June, potatoes fertilized with the lowest N rate (112 kg/ha) were already showing nitrogen deficiency symptoms based on the standard petiole NO_3 test (Table 1). On August 5, petiole NO_3 concentrations in plots with the 224 kg/ha N rate were also below the established range for N sufficiency (Alva, 2004). The rank-order of the petiole NO_3 concentrations show that the four rates of fertilizer application created a range of conditions from nitrogen deficiency to sufficiency throughout the growing season (Table 1), which should be detectable by remote sensing.

On June 22, potatoes with 112 kg/ha applied N had significantly lower chlorophyll concentrations, SPAD values, and leaf area index (Table 1). On August 5, plots with 224 kg/ha applied N had lower chlorophyll concentrations and SPAD readings, but not lower LAI (Table 1).

Flights and image calibrations

While the flight path of the Tetracam Hawkeye sUAS was controlled and logged by autopilot software, the actual sensor position was difficult to control because wind gusts caused the payload frame to sway. Adaption to wind conditions led to many early morning flights, which is not optimal for data acquisition by remote sensing.

Fig. 5. Color-infrared image of the calibration tarps acquired on June 22, 2013. From left to right, the tarps are red, beige, dark blue, gray, and light green (see Fig. 3). Pixel sizes varied between 1 and 4 cm, depending on altitude and view angle. In this image, pixel size was 1.2 cm.

One of the initial sources of error was the color correction matrix included in Tetracam's PixelWrench software. Without the spectral response function of the sensor, the best matrix could not be determined. A new color correction matrix was calculated from the soil spectral response, and the digital numbers for each tarp were reasonable (Fig. 5) based on the previously-measured tarp reflectances from Hunt et al. (2005).

NDVI and GNDVI from the image digital numbers for the tarps were linearly related to the spectral indices calculated from tarp reflectances. Slopes of the DN-NDVI versus reflectance-NDVI (Fig. 6) were about equal for the different dates. However, there were large differences in the intercepts for the DN-NDVI calibrations (Fig. 6A). We thought that differences in incident light intensity were mostly accounted for by normalization (dividing by the sum of the bands), so that variation in the calibration lines would have been caused by differences in either light spectral quality (white balance), degradation of the tarps or the CMOS sensor, or differences in sensor noise caused by air temperature. There was little

progression of the intercepts over time, so degradation of the sensor or tarps probably was not significant.

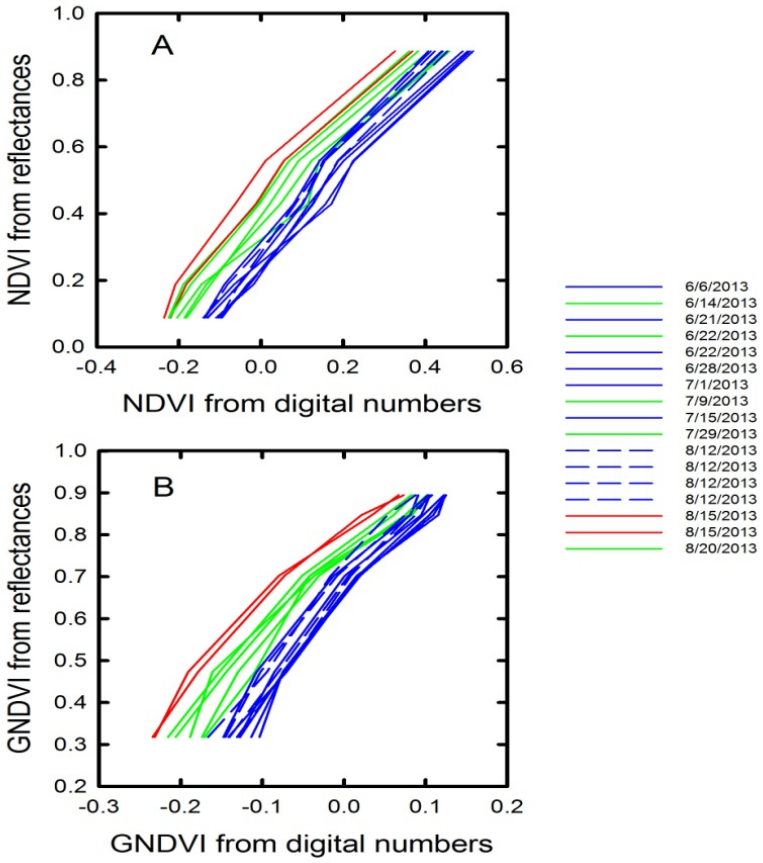

Fig. 6. Comparison of (A) NDVI and (B) GNDVI calculated from tarp digital numbers with the index calculated from tarp reflectances over the 2013 growing season. The line colors indicated the camera exposure times: blue – 172 µs, green – 258 µs, and red – 344 µs. The points are not shown for clarity.

Table 2. Correlation coefficients (r) between the calibration intercepts (Fig. 6) and other variables. The critical r for $\alpha = 0.05$ is 0.456, so all correlations were significant.

	Intercept	Irradiance (W m^{-2})	Temperature (ºC)	Exposure time (µs)
Intercept	1.00			
Irradiance (W m^{-2})	0.781	1.00		
Temperature (ºC)	0.553	0.484	1.00	
Exposure time (µs)	-0.880	-0.854	-0.496	1.00

The intercepts of the NDVI calibrations (Fig. 6A) were highly correlated to camera exposure time and solar irradiance (Table 2). NDVI calibration intercept was less correlated with temperature (Table 2), and was not correlated with either day of the year or time of day (data not shown). Furthermore, the slopes of the

NDVI calibrations were significantly correlated with camera exposure time. Correlations of GNDVI calibration coefficients with exposure time and irradiance were smaller than those for NDVI because the relationships were more non-linear (Fig. 6B).

Sensor calibration is important when comparing data acquired on different dates or different locations. While the ideal goal was calibration of DN to reflectances, calibrated spectral indices from DN can be used to monitor crops over the growing season. Flights at low altitudes with sUAS will need methods of calibration other than an empirical line. Some sensors have up-looking elements to determine incident solar radiation, but unless the directions of the up-looking and down-looking elements are controlled, calibrations for these sensors will be problematic.

Analysis of nitrogen deficiency symptoms with sUAS

Inspection of the images acquired on any single date clearly showed the three plots with 112 kg/ha N applications (Fig. 7). There is more space between the rows for the low N plots compared the other plots, indicating lower vegetation cover. However, determining cover using sampling methods (Booth et al., 2006, 2008) leads to a large range of estimates for a single plot because of a range of view angles from nadir to off-nadir. When the entire plot is averaged together, lower vegetation cover is related to lower NDVI and GNDVI.

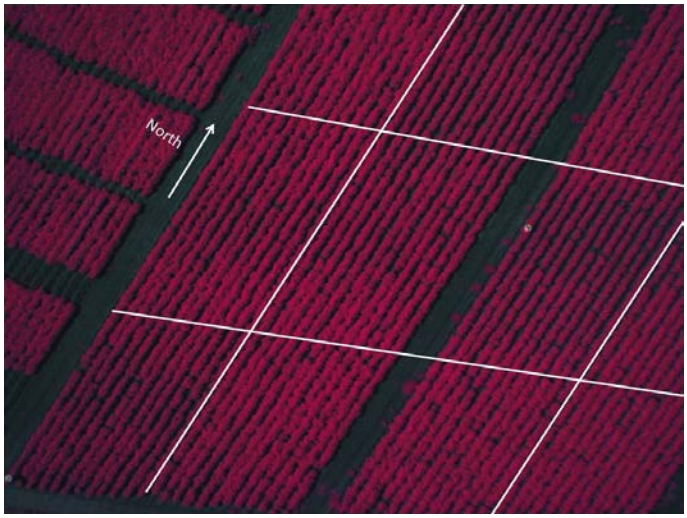

Fig. 7. A color-infrared image acquired on 14 June 2013 selected to show the 3 plots fertilized with low rates of nitrogen (see Fig. 1).

NDVI and GNDVI increased during early vegetative growth, were unchanged during tuber initialization and bulking, and then declined during maturation (Fig. 8A,C). Short-term changes were likely caused by sensor exposure times (Table 2); for example on 26 June, there was a large decrease in both spectral indices (Fig. 8A,C). Unfortunately, this was one date when the calibration tarps were missed during the flight (Fig. 6). We used the camera exposure times recorded in the image metadata to determine the appropriate calibration equation. There was a

large difference between the uncorrected and corrected values of NDVI and GNDVI (Fig. 8), and the spectral indices did not have as much day-to-day variation. The corrections increased the separation of NDVI and GNDVI among treatments (Fig. 8B,D), but only the low N plots (112 kg N/ha) were significantly different from the others.

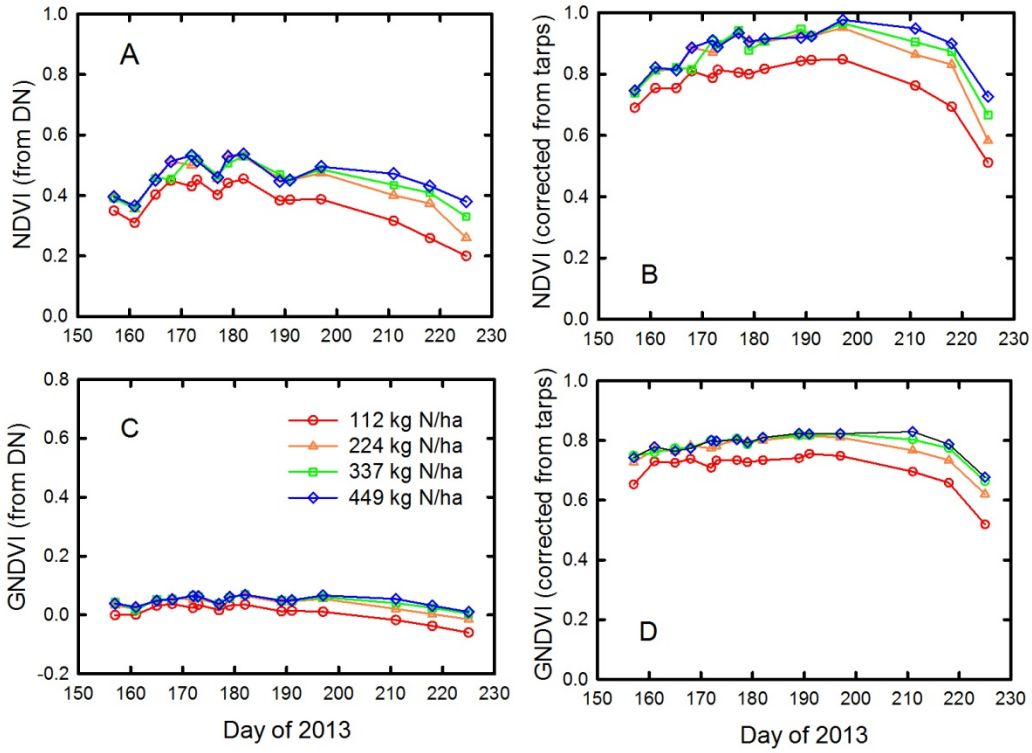

Fig. 8. Change in spectral indices over the 2013 growing season: (A) NDVI calculated from DN; (B) NDVI corrected with tarp calibration equations; (C) GNDVI calculated from DN; and (D) GNDVI corrected with tarp calibration equations. June 22 is day 173 and August 5 is day 217.

Calibration of NDVI and GNDVI using the tarps were needed to compare plots on a single day and within a growing season because of the differences in equations based on the camera exposure time. It is likely that if exposure time was constant, then calibration would not be required to detect differences within a field. However, determining the appropriate management options based on the imagery would difficult without calibration.

From experiments and model simulations, NDVI and similar NIR-red indices have greater sensitivity to biomass, LAI, and fractional vegetation cover, and have less sensitivity to differences in leaf chlorophyll content. Because of the green band, GNDVI is more sensitive to chlorophyll content compared to NDVI (Fig. 4), and may be somewhat less sensitive to LAI. Combination indices (Daughtry et al., 2000; Haboudane et al., 2002) exploit these differences when both leaf area and chlorophyll content are changing.

To determine the contribution of chlorophyll content to the changes in spectral indices, GNDVI was plotted versus NDVI. Based on Fig. 4, GNDVI should decrease more with lower chlorophyll contents relative to NDVI, so a regression line of GNDVI versus NDVI should have a larger slope and a lower intercept. The regression line between GNDVI and NDVI for the 112 kg N/ha treatment followed the prediction (Fig. 9). The differences among the regression equations for the other three treatments were not significantly different (Fig. 9), following the pattern of the measured chlorophyll contents (Table 1).

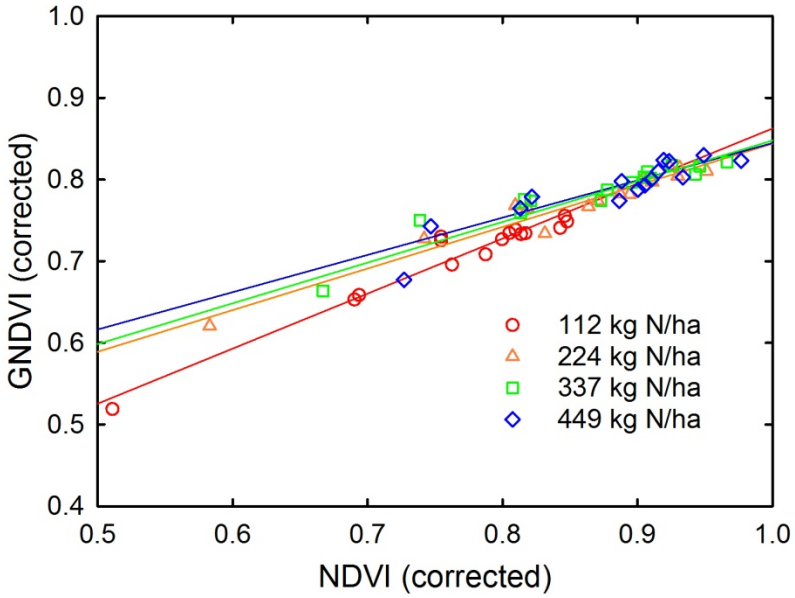

Fig. 9. Comparison of corrected GNDVI and NDVI for separation of the effects of chlorophyll content and LAI.

A combination of the green band and the red band forms another spectral index sensitive to both chlorophyll concentration and LAI; sometimes the index is referred to as the normalized green-red difference index (NGRDI; Tucker, 1979; Hunt et al., 2005). Perhaps because of the problem with the Tetracam ADC color correction matrix, calibrations using the tarps were too variable, so only uncalibrated NGRDI could be compared to the field data (data not shown). Unexpectedly, variation of NGRDI was similar to uncalibrated NDVI (Fig. 8A) and not uncalibrated GNDVI (Fig. 8C). Having sensors with greater spectral resolution will be required to distinguish areas having slow growth caused by nutrient deficiencies from areas having slow growth caused by other stresses. Bands on chlorophyll's red edge (710-730 nm wavelength) have been shown to be more sensitive to smaller differences in chlorophyll concentration compared to visible bands (Hunt et al., 2011, 2013). Low-mass, hyperspectral sensors or multispectral sensors with user selectable bands may become available for sUAS in the near future (Honkavaara et al., 2013).

CONCLUSIONS

The first objective of this study was to establish a baseline for routine sUAS overflights for quantitative monitoring of agriculture. After initial problems with the Tetracam Hawkeye and other sUAS were solved, frequent flights were made and data were acquired. The image data agreed with the field data on the differences of LAI and chlorophyll content among treatments. The most important lesson from the routine data collection was the need for more frequent and thorough calibration of the sensors flown.

There are many sUAS companies being established in response to perceived demand for precision agriculture (Jenkins and Vasigh, 2013); however, the value produced by sUAS for agriculture will be crop information and its relevance to management. We would like to propose the first law of precision agriculture, which is particularly relevant to sUAS, "it's the sensor, not the platform."

DISCLAIMER

Mention of specific products is for identification and does not imply endorsement by the USDA to the exclusion of other suitable products or suppliers.

ACKNOWLEDGMENTS

We thank Ms. Jennifer Hawley for assisting with the image analysis and Dr. Dan Long from the USDA-ARS Columbia Plateau Conservation Research Center for use of their equipment. OSU and USDA-ARS were partially funded by Boeing Research and Technology.

REFERENCES

Alva, L. 2004. Potato nitrogen management. J. Veg. Crop Prod. 10:97-132.

Blackmer, T.M., J.S. Schepers, G.E. Varvel, and G.E. Meyer. 1996. Analysis of aerial photography for nitrogen stress within corn fields. Agron. J. 88:729-733.

Booth, D.T., S.E. Cox, and R.D. Berryman. 2006. Point sampling digital imagery with 'SamplePoint'. Environ. Monit. Assess. 123:97-108.

Booth, D.T., S.E. Cox, T. Meikle, and H.R. Zuuring. 2008. Ground-cover measurements: assessing correlation among aerial and ground-based methods. Environ. Manage. 42:1091-1100.

Daughtry, C.S.T., C.L. Walthall, M.S. Kim, E. Brown de Colstoun, and J.E. McMurtrey, III. 2000. Estimating corn leaf chlorophyll concentration for leaf and canopy reflectance. Remote Sens. Environ. 74:229-239.

Feret, J.B., C. François, G.P. Asner, A.A. Gitelson, R.E. Martin, L.P.R. Bidel, S.L. Ustin, G. le Maire, and S. Jaquemoud. 2008. PROSPECT-4 and 5: Advances in the leaf optical properties model separating photosynthetic pigments. Remote Sens. Environ. 112:3030–3043.

Gitelson, A.A, Y.J. Kaufman and M.N. Merzlyak. 1996. Use of a green channel in remote sensing of global vegetation from EOS-MODIS. Remote Sens. Environ. 58:289-298.

Haboudane, D., J.R. Miller, N. Tremblay, P.J. Zarco-Tejada, and L. Dextraze. 2002. Integrated narrow-band vegetation indices for prediction of crop chlorophyll content for application to precision agriculture. Remote Sens. Environ. 81:416-426.

Herwitz, S.R. L.F. Johnson, S.E. Dunagan, R.G. Higgins, D.V. Sullivan, J. Zheng, B.M. Lobitz, J.G. Leung, B.A. Gallmeyer, M. Aoyogi, R.E. Slye, and J.A. Brass. 2004. Imaging from an unmanned aerial vehicle: agricultural surveillance and decision support. Comput. Electron. Agric. 44:49-61.

Honkavaara, E., H. Saari, J. Kaivosoja, I. Pölönen, T. Hakala, P. Litkey, J. Mäkynen, and L. Pesonen. 2013. Processing and assessment of spectrometric, stereoscopic imagery collected using a lightweight UAV spectral camera for precision agriculture. Remote Sens. 5:5006-5039.

Hunt, E.R., M. Cavigelli, C.S.T. Daughtry, J.E. McMurtrey, and C.L. Walthall. 2005. Evaluation of digital photography from model aircraft for remote sensing of crop biomass and nitrogen status. Precision Agric. 6:359-378.

Hunt, E.R. and C.S.T. Daughtry. 2014. Chlorophyll meter calibrations for chlorophyll content using measured and simulated leaf transmittances. Agron. J. 106:931-939.

Hunt, E.R., C.S.T. Daughtry, J.U.H. Eitel, and D.S. Long. 2011. Remote sensing leaf chlorophyll content using a visible band index. Agron. J. 103:1090-1099.

Hunt, E.R., C.S.T. Daughtry, S.B. Mirsky, and W.D. Hively. In Press. Remote sensing with simulated unmanned aircraft imagery for precision agriculture applications. IEEE J. Sel. Top. Appl. Earth Obs. Remote Sens.

Hunt, E.R., P.C. Doraiswamy, J.E. McMurtrey, C.S.T. Daughtry, E.M. Perry, and B. Akhmedov. 2013. A visible band index for remote sensing leaf chlorophyll content at the canopy scale. Int. J. Appl. Earth Obs. Geoinform. 21:103-112.

Hunt, E.R., W.D. Hively, S.J. Fujikawa, D.S. Linden, C.S.T. Daughtry, and G.W. McCarty. 2010. Acquisition of NIR-green-blue digital photographs from unmanned aircraft for crop monitoring. Remote Sens. 2:290-305.

Jenkins, D. and B. Vasigh. 2013. The Economic Impact of Unmanned Aircraft Systems Integration in the United States. Association for Unmanned Vehicle Systems International, Arlington, VA. http://www.auvsi.org/econreport.

Johnson, D.A., J.R. Alldredge, P.B. Hamm, and B.E. Frazier. 2003. Aerial photography used for spatial pattern analysis of late blight infection in irrigated potato circles. Phytopathology 93:805-812.

Lebourgeois, V., A. Bégue, S. Labbé, B. Mallavan, L. Prévot, and B. Roux. 2008. Can commercial digital cameras be used as multispectral sensors? A crop monitoring test. Sensors 8:7300-7322.

Lelong, C.C.D. P. Burger, G. Jubelin, B. Roux, S. Labbé, and F. Baret. 2008. Assessment of unmanned aerial vehicles imagery for quantitative monitoring of wheat crop in small plots. Sensors 8:3557-3585.

Moran, M.S., G. Fitzgerald, A. Rango, C. Walthall, E. Barnes, W. Bausch, T. Clarke, C. Daughtry, J. Everitt, D. Escobar, J. Hatfield, K. Havstad, T. Jackson, N. Kitchen, W. Kustas, M. McGuire, P. Pinter Jr., K. Sudduth, J. Schepers, T. Schmugge, P. Starks, and D. Upchurch. 2003. Sensor development and radiometric correction for agricultural applications. Photogramm Eng. Remote Sens. 69:705-718.

Tucker, C.J. 1979. Red and photographic infrared linear combinations for monitoring vegetation. Remote Sens. Environ. 8:127-150.

Scharf, P.C. and J.A. Lory. 2002. Calibrating corn color from aerial photographs to predict sidedress nitrogen need. Agron. J. 94:397-404.

Shanahan, J.F. N.R. Kitchen, W.R. Raun, and J.S. Schepers. 2008. Responsive in-season nitrogen management for cereals. Comput. Electron. Agric. 61:51-62.

Wu, J., D. Wang, C.J. Rosen, and M.E. Bauer. 2007. Comparison of petiole nitrate concentrations, SPAD chlorophyll readings, and QuickBird satellite imagery in detecting nitrogen status of potato canopies. Field Crops Res. 101:96-103.

Zhang, C. and J. M. Kovacs. 2012. The application of small unmanned aerial systems for precision agriculture: a review. Precision Agric. 13:693-712.